Single-Component and Mixed Ferrocene-Terminated Alkyl Monolayers Covalently Bound to Si(111) Surfaces

Bruno Fabre* and Fanny Hauquier

Grande Unité "Sciences Chimiques de Rennes", UMR CNRS 6226, Matière Condensée et Systèmes Electroactifs MaCSE, Université de Rennes 1, Campus de Beaulieu, 35042 Rennes Cedex, France

Received: October 6, 2005; In Final Form: February 13, 2006

Self-assembled ferrocene monolayers covalently bound to monocrystalline Si(111) surfaces have been prepared from the attachment of an amine-substituted ferrocene derivative to a pre-assembled acid-terminated alkyl monolayer using carbodiimide coupling. This derivatization strategy yielded nanometer-scale clean, densely packed monolayers, with the ferrocene units being more than 20 Å from the semiconductor surface. The amount of immobilized electroactive units could be varied in the range 2×10^{-11} to $\sim 3.5 \times 10^{-10}$ mol cm^{-2} by diluting the ferrocene-terminated chains by inert *n*-decyl chains. The highest coverage obtained for the single-component monolayer corresponded to 0.25−0.27 bound ferrocene per surface silicon atom. The electrochemical characteristics of the mixed *n*-decyl/ferrocene-terminated monolayers were found to not depend significantly on the surface coverage of ferrocene units. The reversible one-electron wave of the ferrocene/ferrocenium couple was observed at $E^{\circ\prime} = 0.50 \pm 0.01$ V vs SCE, and the rate constant of electron transfer k_{app} was about 50 s^{-1}.

1. Introduction

The functionalization of self-assembled monolayers covalently bound to unoxidized single-crystal and porous silicon surfaces through long alkyl spacers constitutes an attractive approach for designing novel well-defined interfaces for numerous applications, such as molecular electronics, photovoltaic devices, and chemical/biological sensing.[1−3] The two principal methods for producing such functionalized monolayers use the reactions of hydrogen-terminated silicon surfaces with 1-alkenes ω-substituted either directly by functional moieties[4−9] or by reactive groups (acids or esters,[10−33] amines,[14,34−39] alcohols,[11,14,40−43] and semicarbazides[44]), which were subsequently converted to more complex organic or bioorganic structures. Unfortunately, the grafting conditions used in the first method are usually harsh and, consequently, are not applicable for numerous fragile functional structures. In contrast, the second one involves often mild procedures (e.g., aminolysis) to attach the functionality after the grafting step and has been successfully applied to the attachment of numerous biological materials, such as DNA,[10,19,26,32,35,40,42] proteins,[15,31,36,37,44] and enzyme,[38] organic polymers,[20−24,27,28,43] and polyoxometalates.[41] Moreover, another advantage is that the functionalization step takes place on usually well-ordered monolayers while the one-step attachment of ω-substituted 1-alkenes can produce both less ordered and less passivating monolayers, particularly in the case where the ω-substituent is sterically hindered.

Following this approach, we describe, herein, our results on the derivatization of Si(111) surfaces with alkyl monolayers terminated by reversible redox centers, namely ferrocene. These surfaces were produced using a coupling reaction between amino-substituted ferrocene and activated ester groups end-capping an alkyl monolayer. Similar ferrocene-terminated monolayers have been essentially prepared on gold substrates using saturated alkanethiolates[45−64] and conjugated phenylethynyl[65,66,67,68] bridges. These have been extensively used as convenient, robust, and well-defined interfaces for the kinetic and thermodynamic studies of electron transfer, the properties of the electrical double-layer, and the micro-environmental effects on long-range interfacial electron transfer kinetics. Owing to the attractive electrochemical characteristics exhibited by ferrocene (namely, fast electron-transfer rate, low oxidation potential, and stability), its introduction in organic monolayers can also be of interest for the development of electrocatalytic, electroanalysis and biosensing devices, and "wired" enzyme electrodes. Compared to the large number of reports devoted to the ferrocene monolayers bound to gold, the anchoring of this electroactive molecule to silicon substrates has been surprisingly much less developed. However, the hybrid molecule/silicon assemblies offer a number of advantages over molecular assemblies on gold. First, unlike gold, the electronic properties of silicon can be changed by modifying the dopant type and concentration, and by generating electron−hole pairs under illumination. Second, the interfacial Si−C and Si−O bonds are much stronger than the Au−S bond between gold and organosulfur adsorbates, which confer a better stability to these hybrid assemblies.[69] Ferrocene substituted by short vinyl,[70−72] carboxaldehyde,[72] and benzyl alcohol[73−76] linkers have been covalently attached to Si(100) surfaces via the formation of an interfacial Si−C or Si−O bond. The monolayers prepared from ferrocenylbenzyl alcohol exhibited fast electron-transfer rates ($k^\circ > 10^4$ s^{-1} for surface coverages lower than 1×10^{-11} mol cm^{-2}) and long retention-charge times (some tenths of seconds) which render them particularly attractive for charge−storage memory devices.[75,76] The reported values of k° were considerably higher than those obtained at higher surface coverages with the Si−O and Si−C linked monolayers produced from ferrocenecarboxaldehyde and vinylferrocene, i.e., 10 and 130 s^{-1} respectively.[72] These results underline that the redox kinetics of these monolayers is controlled not only by the nature and characteristics

* Corresponding author. Fax: 33 2 2323 6732. Phone: 33 2 2323 6550. E-mail: fabre@univ-rennes1.fr.

10.1021/jp055698n CCC: $33.50
Published on Web 03/16/2006

of the linking group, but also by the coverage which would influence the molecular orientation.[71,72,75] Importantly, the attachment of short-chain ferrocenes to Si(100) surfaces yielded poorly passivating monolayers, which can constitute a serious drawback for long-life applications.[72]

In this paper, Si−C linked monolayers are formed with an aliphatic linker longer than 2 nm between the ferrocene headgroups and the silicon surface. Despite the large use of Si(100) in the semiconductor technology, Si(111) substrates are chosen from which atomically flat monohydride-terminated surfaces can be produced using 40% aq NH_4F,[77,78] and because the alkyl substitution of these surfaces yields usually ordered, densely packed monolayers. By introducing the ferrocene units via the coupling of amino-substituted ferrocene with a *N*-hydroxysuccinimidylundecanoate monolayer, the surface coverage will be governed just by the interaction between the terminal ferrocene moieties and the reactivity of the amine toward the succinimide groups as well. So, the resulting assembly is expected to exhibit characteristics, such as ordering and density, not too different from those of the pre-assembled monolayer, and likely higher than those of a monolayer which would be prepared in one-step from a ferrocene-substituted alkene.[62] Moreover, the dilution of ferrocene-terminated chains by inert *n*-decyl chains enables them to have control over the surface coverage of the electroactive units. The single-component and mixed ferrocene-terminated monolayers have been characterized by various experimental techniques including contact angle goniometry, ellipsometry, AFM, and electrochemistry. The electron-transfer kinetics of the bound ferrocene redox couple has been examined as a function of the surface coverage.

2. Experimental Section

2.1. Reagents. Acetone (min. 99.8%, Carlo Erba), methanol (min. 99.9%, Carlo Erba), dichloromethane (anhydrous analytical grade, SDS), and 1,1,1-trichloroethane (99+%, A.C.S. reagent, Aldrich) were used without further purification. Acetonitrile from SDS was distilled over calcium hydride before use. The chemicals used for cleaning and etching of silicon wafer pieces (30% H_2O_2, 96−97% H_2SO_4, and 40% NH_4F solutions) were of semiconductor grade (Riedel-de-Haën). Ethyl undecylenate (Aldrich, 97%) was passed through a neutral, activated alumina column to remove residual water. 1-Decene (Fluka, >95%) was passed through a neutral, activated alumina column, distilled over sodium, and stored under argon. *N*-hydroxysuccinimide NHS (Acros, 98+%) and 1-(3-dimethylaminopropyl)-3-ethylcarbodiimide EDC (Acros, 98+%) were used as received.

2-Aminoethylferrocenylmethylether (**1**) was synthesized in one step from commercially available (ferrocenylmethyl)trimethylammonium iodide (Strem Chemicals, 99%) following a previously reported procedure.[79] Briefly, the reaction of (ferrocenylmethyl)trimethylammonium iodide with ethanolamine gave **1** in 50% yield.

2.2. Covalent Attachment of the Single-Component and Mixed Ferrocene-Terminated Monolayers on Silicon. A single side polished silicon(111) shard (1.5×1.5 cm^2, 1−5 Ω cm, *p*-type, boron doped, thickness = 525 ± 25 μm, Siltronix) was sonicated for 10 min successively in acetone, methanol, and ultrapure 18.2 MΩ cm water. It was then cleaned in 3:1 v/v concentrated H_2SO_4/30% H_2O_2 at 100 °C for 30 min, followed by copious rinsing with ultrapure water.

Caution: *The concentrated H_2SO_4:H_2O_2 (aq) piranha solution is very dangerous, particularly in contact with organic materials, and should be handled extremely carefully.*

The surface was etched with ppb grade 40% aqueous argon-deaerated NH_4F for 15 min to obtain atomically flat Si(111)−H.[78] It was then dipped in argon-deaerated ultrapure water for several seconds, dried under an argon stream, and transferred immediately into a Pyrex Schlenk tube containing ca. 10 mL of ethyl undecylenate or ethyl undecylenate/1-decene mixture, previously deoxygenated at 100 °C for 3 h at least. Temperature was increased to 115−120 °C and kept at this value overnight. After cooling to 40−50 °C, the ester-modified silicon surface was rinsed copiously with dichloromethane and 1,1,1-trichloroethane, and dried under an argon stream. The conversion of the ester to carboxylic acid moieties was performed using a procedure described by Strother et al.[26] The surface was dipped in a 0.25 M solution of potassium *tert*-butoxide (*t*-BuOK) in DMF for 10 min at room temperature, then transferred in 1 M aq HCl for 10 min and rinsed with water.

The terminal COOH groups were activated with NHS by immersing the modified silicon surface for 2 h in a freshly prepared mixture of a deaerated solution of EDC at 0.2 M in water (2.5 mL) and a deaerated solution of NHS at 0.1 M in water (2.5 mL). The mixture was gently purged by bubbling with inert gas. The surface was then rinsed with water, dried under an argon stream and used immediately for amide formation.

The covalent attachment of ferrocene redox units on Si(111) was performed by immersing the NHS-activated silicon surface in a deaerated dichloromethane solution containing 5×10^{-2} M of **1** at room temperature for 3 h. The ferrocene-modified surface was rinsed with dichloromethane and 1,1,1-trichloroethane, and dried under an argon stream.

2.3. Surface Characterization. XPS measurements were performed using a VSW HA100 system with MgKα photons at 54° incidence and a 45° takeoff angle. This angle is used to increase surface sensitivity, especially to check for Si−O bonds appearance. Spectra were fitted with a convolution of Lorentzian and Gaussian profiles using standard procedures.

AFM images were recorded with a PicoSPM II microscope from Molecular Imaging using conventional gold coated−silicon nitride (contact mode) tips from Scientec.

The thickness of the organic monolayer was estimated using a Jobin−Yvon model Ellisel ellipsometer with a HeNe laser and an angle of incidence of 70°. The refractive index of the monolayer was set at $n = 1.46$ and $n = 3.85$, and $k = 0.02$ were used for the silicon substrate, where k is the optical constant of silicon. Uncertainty ±1 Å.

Water contact angles were measured with a homemade goniometer under ambient conditions using a horizontal light beam to illuminate the liquid droplet. Uncertainty ±2°.

2.4. Electrochemical Characterizations. The cyclic voltammetry and differential capacitance measurements were performed with an Autolab electrochemical analyzer (PGSTAT 20 potentiostat/galvanostat from Eco Chemie B.V., equipped with the GPES/FRA software) in a self-designed three-electrode Teflon cell. The working electrode, modified Si(111), was pressed against an opening in the cell bottom using a Viton O-ring seal. An ohmic contact was made on the previously polished rear side of the sample by applying a drop of an In−Ga eutectic (Alfa-Aesar, 99.99%). The electrochemically active area of the Si(111) surface (namely, 1.1 cm^2) was estimated by measuring the charge under the voltammetric peak corresponding to the ferrocene oxidation on Si(111)−H and comparing this value to that obtained with a 1 cm^2-Pt electrode under the same conditions. The counter electrode was a platinum foil and the system 10^{-2} M Ag^+ | Ag in acetonitrile was used as the

SCHEME 1. Preparation of the Ferrocene-terminated Alkyl Monolayers Bound to Si(111) Surfaces

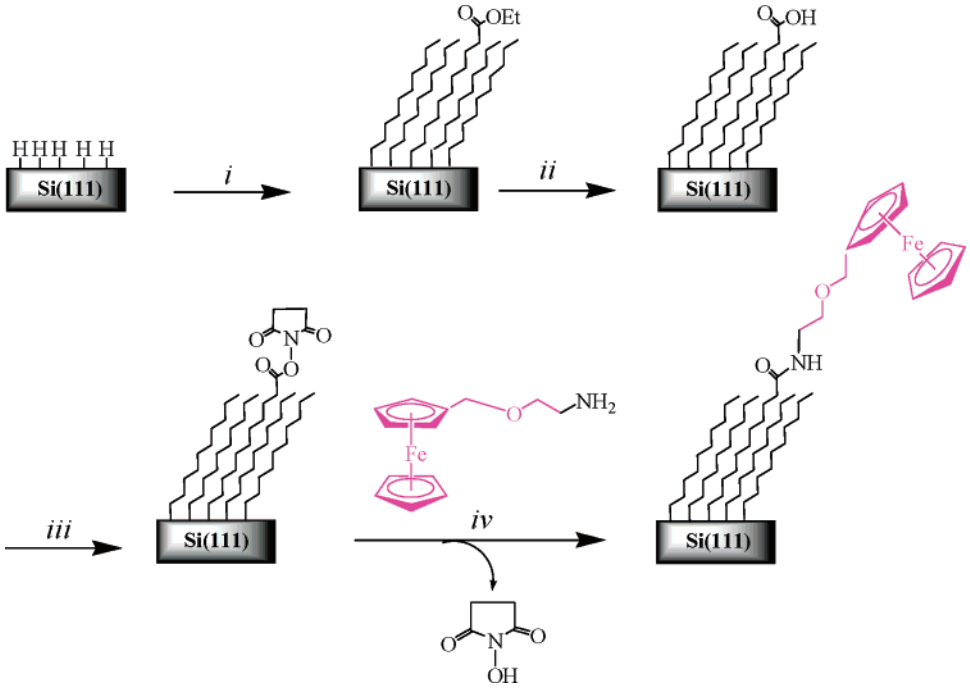

Reagents and Conditions: (*i*) Neat ethyl undecylenate or mixture of ethyl undecylenate and 1-decene, 120 °C, 20 h; (*ii*) DMF/0.25 M *t*-BuOK, rt, 10 min, then 1 M HCl, rt, 10 min; (*iii*) 0.1 M aq. NHS + 0.2 M aq. EDC, rt, 2 h; (*iv*) CH_2Cl_2/0.05 M **1**, rt, 3 h.

reference electrode (+0.29 V vs aqueous SCE or −0.09 V vs ferrocene/ferrocenium). All reported potentials are referred to SCE (uncertainty ±0.01 V). Tetra-*n*-butylammonium perchlorate Bu_4NClO_4 was purchased from Fluka (puriss, electrochemical grade). The (CH_3CN + 0.1 M Bu_4NClO_4) electrolytic medium was dried over activated, neutral alumina (Aldrich) for 30 min, under stirring and under argon. About 20 mL of this solution was transferred with a syringe into the electrochemical cell prior to experiments.

All electrochemical measurements were carried out inside a homemade Faraday cage at room temperature (20 ± 2 °C) and under a constant flow of argon. Solution resistance was compensated by positive feedback.

3. Results and Discussion

3.1. Single-Component Ferrocene-Terminated Alkyl Monolayer. The covalent derivatization of Si(111) surfaces by a ferrocene-functionalized monolayer is depicted in Scheme 1. In the first step, the thermal reaction at 120 °C under argon of hydrogen-terminated silicon (Si−H)[11,34,80,81] with neat ethyl undecylenate results in a Si−C linked organic monolayer terminated by functionalizable ester groups.[14] The treatment of the modified silicon surface with *t*-BuOK then HCl leads to the conversion of the terminal units into carboxyl groups.[26] This procedure has been reported to be more efficient to hydrolyze the esters than the alternate method using boiling acid baths (e.g., concentrated HCl) for several hours.[11,14] After NHS activation of the monolayer,[16,17,19] the ferrocene units were introduced using the amidation reaction with 2-aminoethylferrocenylmethylether.[79]

The thicknesses measured by ellipsometry of the initial ester- and ferrocene-terminated monolayers were 16 and 26 Å, respectively. From calculations of energy minimization using the semiempirical PM3 method, the lengths of the ester- and ferrocene-terminated molecular chains have been estimated at 17 and 28 Å, respectively, with the ferrocene units being lifted up. These values give tilt angles of ca. 20° from the surface normal for the two monolayers, which would indicate that the chemical modification of the headgroups does not significantly change the orientation of the organic chains. As has already been demonstrated by Sieval et al. from molecular modeling simulations,[11] the presence of a terminal ester group results in a considerably less tilted monolayer compared to that produced from simple unfunctionalized 1-alkenes. Static contact angles measured with water reveal, as expected, that the acid-modified surface is more hydrophilic than the ester- and ferrocene-modified surfaces, 45 ± 2° vs 73 ± 2° and 71 ± 2°, respectively.

The XPS analysis of the monolayer-modified silicon surface reveals characteristic peaks from the silicon substrate itself and from the C 1s, O 1s, N 1s, and Fe 2p core levels of the attached organic molecule (see Supporting Information). The high-resolution C 1s peak can be decomposed into three components at 285.0, 287.0, and 289.2 eV. The first one corresponds to unresolved contributions from both aromatic and polymethylene carbons, whereas the weaker peaks at 287.0 and 289.2 eV are reasonably attributed to heteroelement-bound carbons (*C*-O, *C*-N) and amide carbon (*C*(O)NH), respectively. The Fe 2p spectrum is composed of two peaks at 708.4 and 721.0 eV, corresponding to the Fe $2p_{3/2}$ and Fe $2p_{1/2}$ signals, these values being perfectly consistent with those previously published for ferrocene.[82,83] Moreover, the formation of silicon oxides resulting from the reaction of remained silicon hydrides with residual oxygen is not detected (i.e., absence of a peak at binding energy 102−104 eV). The absolute surface coverage of the single-component ester-terminated monolayer is estimated at 0.50 ± 0.05 per surface silicon atom from the procedure developed by Cicero et al. combining XPS data with ellipsometric measurements.[84] The photo-electron mean-free path parameters for the ester monolayer and silicon substrate, which are involved in the analysis are the same as those used by Cicero et al. So, the value of ca. 0.50 would be consistent with a maximum coverage of Si(111), as a theoretical limit of about 50% has been proposed by Linford et al.[80] However, it must be pointed out that the uncertainty in the determination of this coverage is estimated

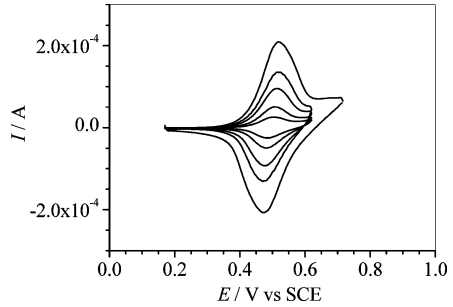

Figure 1. Cyclic voltammograms at 0.1, 0.2, 0.4, 0.6, and 1 V s^{-1} of the single-component ferrocene-terminated monolayer in CH_3CN + 0.1 M Bu_4NClO_4.

at ±30−50% because the attenuation lengths of photoelectrons used in the analysis have been measured for hydrocarbon films. From the ATR−FTIR spectroscopy, a coverage of 0.30−0.40 has been reported for the same ester monolayer.[14]

Typical cyclic voltammograms of the ferrocene-terminated monolayer in CH_3CN + 0.1 M Bu_4NClO_4 are shown in Figure 1 as a function of the potential scan rate v. The reversible one-electron wave of the ferrocene/ferrocenium couple is clearly visible at $E^{\circ\prime} = 0.50 \pm 0.01$ V vs SCE. In solution, ferrocene is oxidized at 0.41 and 0.37 V vs SCE onto platinum and Si(111)−H, respectively. So, the positive ca. 100 mV-shift observed for bound ferrocene can be ascribed either to the stabilization of ferrocene relative to ferrocenium by being incorporated in a hydrophobic environment created by the organic chains, or to the electron-withdrawing character of the underlying amide bonds making the ferrocene more difficult to oxidize. As expected for surface-confined redox species,[85] the peak-to-peak separation ΔE_p measured at 0.1 V s^{-1} is close to zero (20 mV), the ratio of anodic to cathodic peak currents (I_{pa}/I_{pc}) is close to unity and the peak currents are proportional to the potential scan rates. Moreover, the full-width at half-maximum (fwhm) is found to be 105 mV, that is higher than 90 mV predicted theoretically,[85] indicating the presence of some weak lateral interactions between the molecules in these films. Under inert atmosphere conditions, repeated scanning between the reduced and oxidized forms of ferrocene results in a decrease of the peak currents lower than 10% after 10^4 cycles. The total amount Γ of attached ferrocene units can be estimated at (3.3−3.5) × 10^{-10} mol cm^{-2} from the area under either the anodic or cathodic peak at low scan rates, i.e., 0.05−0.2 V s^{-1}. This value corresponds to a surface coverage of 0.25−0.27 ferrocene per surface silicon atom considering that the atomic density of Si(111) is 7.8 × 10^{14} atoms cm^{-2}.[86] A specific area of about 50 $Å^2$ per bound ferrocene can thus be deduced, which is somewhat greater than 35 $Å^2$ calculated by considering the ferrocene molecules as spheres with a diameter of 6.6 Å.[45] This indicates a reasonably dense packing of the ferrocene-terminated chains. It must be noted that the surface coverage determined in this work compares well with the values obtained for the monolayers of ferrocenylbenzyl alcohol[75] and vinylferrocene[72] covalently bound to Si(100) surfaces, i.e., 4.2 × 10^{-10} and 2.4 × 10^{-10} mol cm^{-2} respectively.

To obtain further insights on the electrical properties of ferrocene-modified Si(111) surfaces, differential capacitance measurements have been performed. Figure 2 shows the differential capacitance C vs potential E curves measured at different frequencies of the electroactive monolayer in contact with CH_3CN + 0.1 M Bu_4NClO_4. Peaks are observed at 0.5 V and their amplitude increases with decreasing the measurement frequency. These peaks are related to the oxidation of bound ferrocene units and their position coincides with $E^{\circ\prime}$ determined

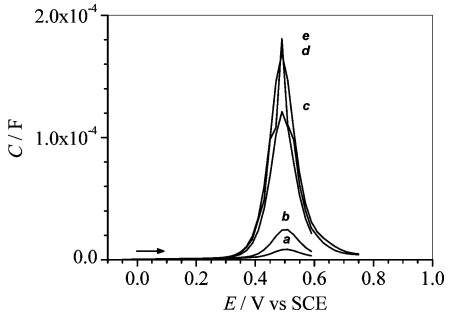

Figure 2. Capacitance-potential curves of the single-component ferrocene-terminated monolayer in CH_3CN + 0.1 M Bu_4NClO_4 measured at (a) 1000, (b) 500, (c) 100, (d) 50, and (e) 25 Hz.

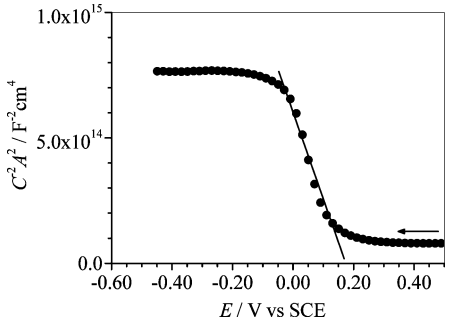

Figure 3. Mott−Schottky plot (C^{2-} vs E) at 50 kHz of the single-component ferrocene-terminated monolayer in CH_3CN + 0.1 M Bu_4NClO_4.

by cyclic voltammetry, as expected for adsorbed, reversible redox monolayers.[87] Furthermore, the maximum capacitance of about 140−150 μF cm^{-2} measured for frequencies lower than 50 Hz demonstrates the high charge-storage capacity of our hybrid device. For potentials lower than 0.2 V, the capacitance of the redox system can be described following the Mott−Schottky equation (C^{2-} vs E, eq 1), which is a measure of the space-charge layer under depletions conditions.[88] where ϵ is the

$$C^{-2} = \frac{2}{q\epsilon\epsilon_0 N_d A^2}\left(E - E_{fb} - \frac{kT}{q}\right) \qquad (1)$$

relative permittivity of silicon (11.7), ϵ_0 is the permittivity of free space, N_d is the dopant density of the semiconductor, A is the area of the electrode, E_{fb} is the flat-band potential of the semiconductor electrode, k is the Boltzmann constant, T is temperature, and q is the electronic charge. A linear $C^{2-} - E$ plot is obtained over the potential range 0.15 to −0.10 V (Figure 3), the slope and the intercept of which enable the flat-band potential and the dopant density to be determined. N_d is estimated at 3.5 × 10^{15} cm^{-3} and is consistent with the dopant density derived from the four-probe resistivity measurements of this same silicon sample. The value calculated for E_{fb} (0.20 V) is also in good agreement with other electrochemical data reported for HF-treated p-doped silicon.[89] This indicates that there is no surface dipole at the silicon-alkyl interface, as expected from the weak polarization of the Si−C bond.

3.2. Mixed *n*-Decyl/Ferrocene-Terminated Monolayers. Effect of the Coverage on the Electrochemical Characteristics of Bound Ferrocene. The surface coverage of ferrocene-terminated chains can be adjusted by diluting ethyl undecylenate with an unreactive 1-alkene (namely, 1-decene). Co-reaction with 1-decene allows the C_{11} ester group to protrude above the plane of methyl groups. This has the beneficial effects of minimizing the disruption of the alkyl chain packing in the monolayers and allowing access to the ester group by reagents.

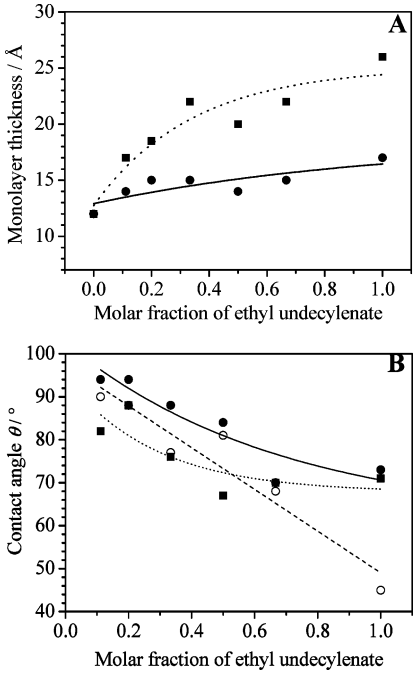

Figure 4. (A) Ellipsometric thickness and (B) water contact angle of the decyl monolayer mixed with the (●, solid line) ester-, (○, dashed line) acid-, or (■, dotted line) ferrocene-terminated monolayer as a function of the molar fraction of ethyl undecylenate in the initial mixture of two alkenes.

Moreover, it has been demonstrated that the ratio of the two chains on the Si(111) surface was almost the same as their molar ratio in the solution.[14]

As expected, the ellipsometric data show that the thicknesses of the two-component monolayers increase monotonically from the length of decene (12 Å) to about the length of the ester- (16 Å) or ferrocene- (26 Å) terminated monolayer as the molar fraction of ethyl undecylenate is increased (Figure 4A). Additionally, the water contact angle measurements reveal that the hydrophobicity of the surfaces decreases gradually with the ester concentration. However, the decrease observed for the mixed decyl/acid-terminated monolayers is much stronger than that obtained for the mixed decyl/ester- or decyl/ferrocene-terminated monolayers (Figure 4B). This is related to much larger differences in wetting behavior between methyl- and COOH-terminated chains, compared with methyl/ester or methyl/ferrocene systems. For surfaces with fractional areas of different wettabilities as those studied here, a linear relationship between the cosine of the contact angle θ and the surface molar fraction of the ester χ_{ester}^{surf} is predicted theorically (Cassie's law, eq 2)[90] where θ_{dec} and θ_{ester} are the angle contact values determined for pure decyl and ethyl undecylate monolayers. As displayed in Figure 5, a plot of cosθ against the molar fraction of ethyl undecylenate in solution χ_{ester}^{soln} is approximately linear, which indicates that the solution and surface compositions are close to each other, in agreement with the results reported by others derived from IR spectroscopic data.[14,29] Such a linear correlation was also observed by Zuilhof and co-workers with mixed *n*-alkyl/amino-[34] and *n*-alkyl/fluoro-[91] terminated monolayers on silicon.

$$\cos\theta = (\cos\theta_{ester} - \cos\theta_{dec})\,\chi_{ester}^{surf} + \cos\theta_{dec} \qquad (2)$$

The AFM analysis of the modified surfaces shows a structure identical to that of Si(111)−H, with atomically flat, defect-free terraces separated by about 3 Å-high steps (Figure 6). The

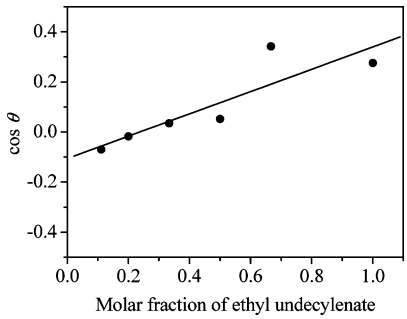

Figure 5. Cosine of the water contact angle of the mixed *n*-decyl/ester-terminated monolayers as a function of the molar fraction of ethyl undecylenate in the initial mixture of two alkenes (Cassie plot). The straight line has been plotted following eq 2 with $\theta_{dec} = 98°$ and $\theta_{ester} = 73°$.

measured root-mean-square (rms) roughness is about 3.5 Å and not dependent on the composition of the mixed monolayers. Moreover, any contrast in friction images is not observed and any adventitious material is not removed upon a prolonged AFM tip scanning on the same place. Therefore, the surfaces appear perfectly clean whatever the coverage of ferrocene units.

The electrochemical characteristics of the mixed *n*-decyl/ferrocene-terminated monolayers are found to not depend significantly on the surface coverage of ferrocene units. Obviously, the anodic and cathodic peak currents corresponding to the reversible ferrocene oxidation−reduction process increase with the molar fraction of ethyl undecylenate in solution. However, the values of $E^{\circ\prime}$ and fwhm are found to be constant at 0.50 ± 0.01 V vs SCE and 105 ± 20 mV respectively, and very similar to those obtained for the single-component ferrocene monolayer. Additionally, E_{fb} extracted from capacitance measurements does not change with the surface coverage. Figure 7 shows representative cyclic voltammograms for three different mixed monolayers at scan rates ranging from 0.1 to 1 V s^{-1}. Upon a repetitive scanning at 0.1 V s^{-1}, the surfaces show an electroactivity loss similar to that observed for the single-component monolayer, i.e., 10−15% after 10^4 cycles. It must be noticed that these modified Si(111) surfaces do not show any degradation when stored in an inert argon atmosphere for several weeks. Nevertheless, surface oxidation occurs when they are either stored in the laboratory atmosphere or in a not thoroughly dried organic medium, as proved by the appearance of numerous triangular pits in the AFM images and the presence of a peak of surface states in the *C* vs *E* curves. Furthermore, the stability of the mixed monolayers under such conditions is found to not depend significantly on their composition. The amount of attached ferrocene units estimated from low scan rate cyclic voltammograms can be plotted against the molar fraction of ethyl undecylenate (Figure 8). A linear correlation is expected provided that the overall conversion of the ester to ferrocene terminal groups is constant and the total coverage of the Si(111)−H surface by the *n*-decyl and ethyl undecylate chains is not dependent on the composition of the alkene mixture. The deviation from linearity observed in Figure 8 is thought to be ascribed to a decrease in the yield of the amidation reaction due to increasing steric effects in the mixed monolayers which render difficult the approach of the amine-substituted ferrocene. The variation of cyclic voltammograms with υ for different mixed monolayers is consistent with the presence of a surface-confined redox species, as proved by the linear relationship between the peak currents and υ over a large range of scan rates, i.e., from 0.1 to 100 V s^{-1} (Figure 9A).[85] Upon increasing the potential scan rate, the peak potentials shift in positive and negative directions relative to $E^{\circ\prime}$ which reflects

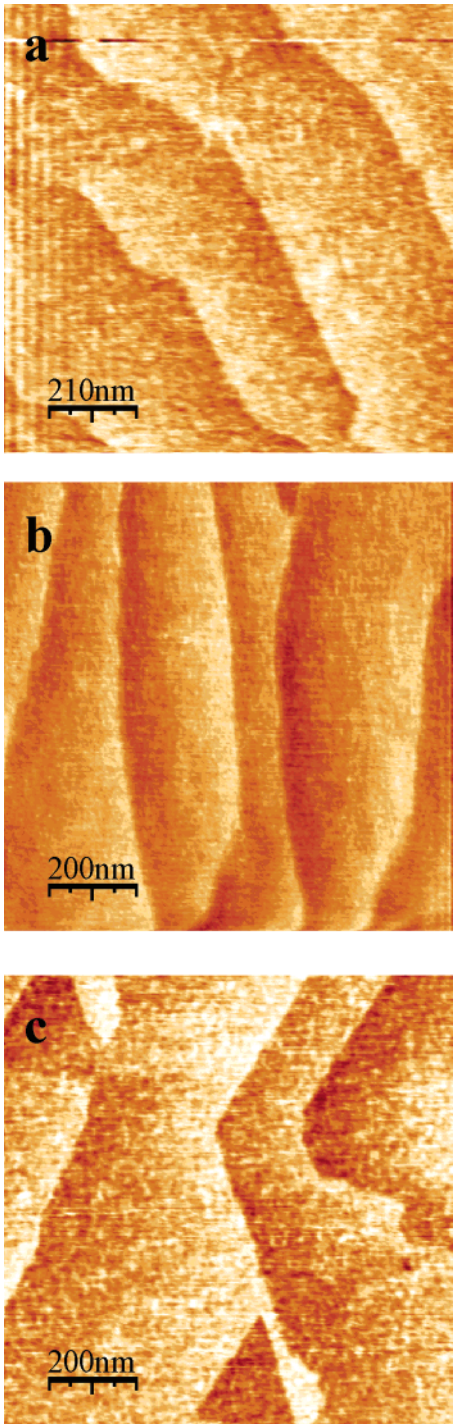

Figure 6. Contact-mode ($1 \times 1\ \mu m^2$) AFM images for (a) Si(111)−H and (b,c) the mixed *n*-decyl/ferrocene-terminated monolayers prepared from (b) 11 and (c) 67 mol. % ethyl undecylenate.

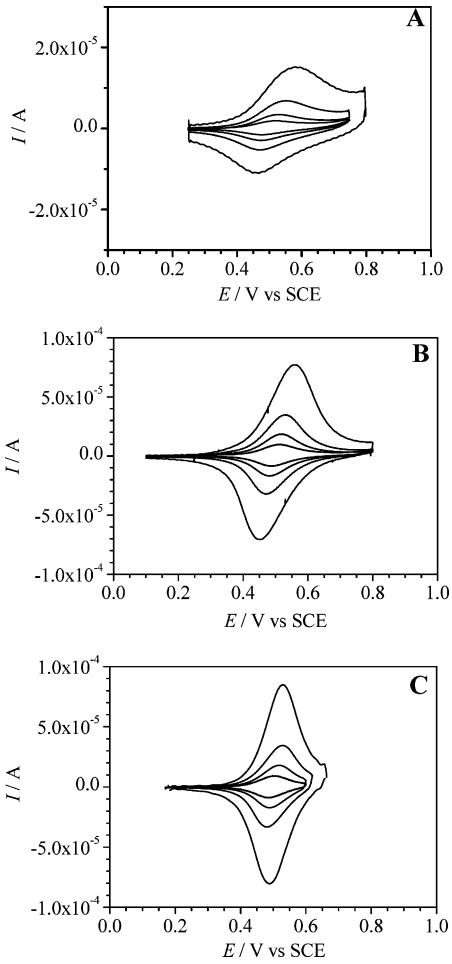

Figure 7. Cyclic voltammograms in CH_3CN + 0.1 M Bu_4NClO_4 of the mixed *n*-decyl/ferrocene-terminated monolayers prepared from different alkene mixtures containing (A) 11, (B) 33, and (C) 50 mol. % ethyl undecylenate. Potential scan rates: 0.1, 0.2, 0.4, and 1 V s^{-1}.

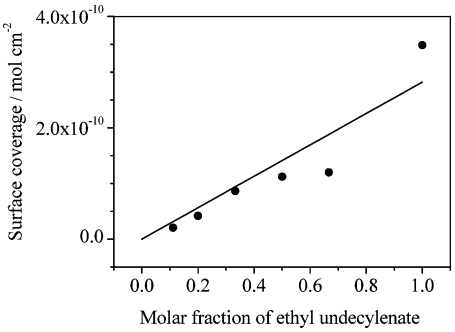

Figure 8. Variation of the surface coverage of ferrocene in the mixed monolayers with the molar fraction of ethyl undecylenate in the initial alkene mixture.

control of the voltammetry by the rate of electron transfer of the ferrocene units (Figure 9B). Apparent rate constants for electron transfer, k_{app}, was calculated using Laviron's formalism (eq 3)[92] based on the classical Butler−Volmer theory.

$$k_{app} = (1\text{-}\alpha)nF\upsilon_a/RT \qquad (3)$$

where α is the charge-transfer coefficient and υ_a is the intersect of the two linear regions in the graph E_{pa} vs logυ obtained at low and high scan rates. The symmetry between the anodic and cathodic branches suggests that α is 0.5. The k_{app} values calculated for the mixed and the single-component ferrocenyl monolayers at surface coverages ranging from 2×10^{-11} to 3.5×10^{-10} mol cm^{-2} are plotted in Figure 10. Despite the visible dispersion in the k_{app} values, k_{app} appears to not vary significantly with Γ but rather to converge to a nearly constant value of $\sim 50 \pm 10\ s^{-1}$. Similar rate constants have been calculated by treating the voltammetric data with the Marcus model instead of Laviron's formalism.[93] In the range of coverages investigated herein, the invariance of k_{app} with coverage implies that the orientation of the ferrocene-terminated chains does not change with coverage and/or the diluent decyl chains do not impede the ferrocene-terminated chain motion. Similar trends have been previously reported for ferrocene and porphyrin redox monolayers on Si(100) surfaces at high

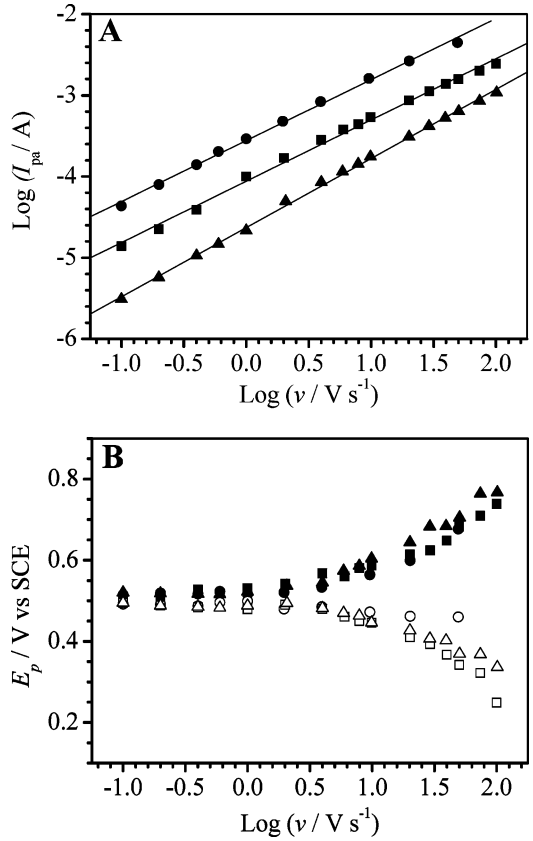

Figure 9. (A) LogI_{pa} − log$v$ and (B) E_p − log$v$ plots determined from cyclic voltammograms in CH_3CN + 0.1 M Bu_4NClO_4 of the mixed *n*-decyl/ferrocene-terminated monolayers. Surface coverage of ferrocene: (●) 3.5×10^{-10}, (■) 1.1×10^{-10}, and (▲) 0.4×10^{-10} mol cm^{-2}. The lines are linear fits and the corresponding correlation coefficients range from 0.995 to 0.999. E_{pa} and E_{pc} are depicted as filled and unfilled symbols, respectively.

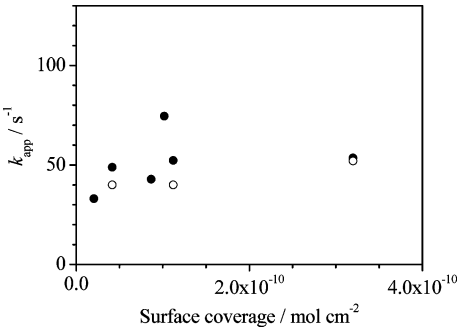

Figure 10. Apparent electron-transfer rate constants for ferrocene as a function of the surface coverage. k_{app} was determined (●) graphically from E_p − log$v$ plots using Laviron's formalism or (○) using the Marcus model.

coverages[72,75] while at very low coverages (typically, between 10^{-12} and 10^{-11} mol cm^{-2}), k_{app} decreased monotonically as the surface coverage increased.[75]

4. Conclusions

Neat and diluted ferrocene-terminated monolayers studied in this work showed electron-transfer characteristics essentially independent of the surface coverage of the ferrocene centers. For those hybrid assemblies, the dilution with *n*-decyl chains offers the advantages of controlling the amount of attached electroactive centers without changing significantly both the rate of electron transfer and the structure of the monolayer. This situation was thought to result from the attachment strategy of ferrocene on the Si(111) surface. Indeed, ferrocene was attached covalently on a reactive mixed monolayer containing a long alkyl linker which was previously formed from hydrogen-terminated Si(111). This procedure ensures that the organization and the packing of the preassembled monolayer are not too affected after the ferrocene anchoring. In the case of the direct adsorption of reactive ferrocene on gold[45,57] or silicon(100)[72,75] substrates, the orientation of the electroactive molecule on the surface may change with the surface coverage and the resulting mixed monolayers may be of varying quality. Moreover, the two-step attachment strategy provides a favorable chemical environment to protect efficiently the semiconductor surface against the permeation of solvent, counterions, and other species susceptible to damage it.

Acknowledgment. F. Solal and S. Ababou-Girard (PALMS, UMR CNRS n°6627, University of Rennes 1, France) are fully acknowledged for XPS measurements.

Supporting Information Available: XPS survey and high-resolution spectra of a freshly prepared single-component ferrocene-terminated monolayer. This material is available free of charge via the Internet at http://pubs.acs.org.

References and Notes

(1) Buriak, J. M. *Chem. Rev.* **2002**, *102*, 1271−1308.
(2) Wayner, D. D. M.; Wolkow, R. A. *J. Chem. Soc., Perkin Trans. 2* **2002**, 23−34.
(3) Bent, S. F. *J. Phys. Chem. B* **2002**, *106*, 2830−2842.
(4) de Smet, L. C. P. M.; Stork, G. A.; Hurenkamp, G. H. F.; Sun, Q.-Y.; Topal, H.; Vronen, P. J. E.; Sieval, A. B.; Wright, A.; Visser, G. M.; Zuilhof, H.; Sudhölter, E. J. R. *J. Am. Chem. Soc*. **2003**, *125*, 13916−13917.
(5) Pike, A. R.; Patole, S. N.; Murray, N. C.; Ilyas, T.; Connolly, B. A.; Horrocks, B. R.; Houlton, A. *Adv. Mater*. **2003**, *15*, 254−257.
(6) Yamanoi, Y.; Yonezawa, T.; Shirahata, N.; Nishihara, H. *Langmuir* **2004**, *20*, 1054−1056.
(7) Altavilla, C.; Ciliberto, E.; Gatteschi, D.; Sangregorio, C. *Adv. Mater.* **2005**, *17*, 1084−1087.
(8) Boiadjiev, V. I.; Brown, G. M.; Pinnaduwage, L. A.; Goretzki, G.; Bonnesen, P. V.; Thundat, T. *Langmuir* **2005**, *21*, 1139−1142.
(9) Yamanoi, Y.; Yonezawa, T.; Shirahata, N.; Nishihara, H. *Langmuir* **2004**, *20*, 1054−1056.
(10) Wagner, P.; Nock, S.; Spudich, J. A.; Volkmuth, W. D.; Chu, S.; Cicero, R. L.; Wade, C. P.; Linford, M. R.; Chidsey, C. E. D. *J. Struct. Biol.* **1997**, *119*, 189−201.
(11) Sieval, A. B.; Demirel, A. L.; Nissink, J. W. M.; Linford, M. R.; van der Maas, J. H.; de Jeu, W. H.; Zuilhof, H.; Sudhölter, E. J. R. *Langmuir* **1998**, *14*, 1759−1768.
(12) Sun, Q.-Y.; de Smet, L. C. P. M.; van Lagen, B.; Wright, A.; Zuilhof, H.; Sudhölter, E. J. R. *Angew. Chem., Int. Ed.* **2004**, *43*, 1352−1355.
(13) Sun, Q.-Y.; de Smet, L. C. P. M.; van Lagen, B.; Giesbers, M.; Thüne, P. C.; van Engelenburg, J.; de Wolf, F. A.; Zuilhof, H.; Sudhölter, E. J. R. *J. Am. Chem. Soc*. **2005**, *127*, 2514−2523.
(14) Boukherroub, R.; Wayner, D. D. M. *J. Am. Chem. Soc.* **1999**, *121*, 11513−11515.
(15) Wojtyk, J. T. C.; Morin, K. A.; Boukherroub, R.; Wayner, D. D. M. *Langmuir* **2002**, *18*, 6081−6087.
(16) Boukherroub, R.; Wojtyk, J. T. C.; Wayner, D. D. M.; Lockwood, D. J. *J. Electrochem. Soc.* **2002**, *149*, H59−H63.
(17) Mitchell, S. A.; Ward, T. R.; Wayner, D. D. M.; Lopinski, G. P. *J. Phys. Chem. B* **2002**, *106*, 9873−9882.
(18) Boukherroub, R.; Petit, A.; Loupy, A.; Chazalviel, J.-N.; Ozanam, F. *J. Phys. Chem. B* **2003**, *107*, 13459−13462.
(19) Voicu, R.; Boukherroub, R.; Bartzoka, V.; Ward, T.; Wojtyk, J. T. C.; Wayner, D. D. M. *Langmuir* **2004**, *20*, 11713−11720.
(20) Fabre, B.; Lopinski, G. P.; Wayner, D. D. M. *Chem. Commun.* **2002**, 2904−2905.
(21) Fabre, B.; Lopinski, G. P.; Wayner, D. D. M. *J. Phys. Chem. B* **2003**, *107*, 14326−14335.
(22) Fabre, B.; Wayner, D. D. M. *Langmuir* **2003**, *19*, 7145−7146.
(23) Fabre, B.; Wayner, D. D. M. *J. Electroanal. Chem.* **2004**, *567*, 289−295.
(24) Fabre, B.; Ababou-Girard, S.; Solal, F. *J. Mater. Chem.* **2005**, *15*, 2575−2582.

(25) Asanuma, H.; Lopinski, G. P.; Yu, H.-Z. *Langmuir* **2005**, *21*, 5013−5018.
(26) Strother, T.; Cai, W.; Zhao, X.; Hamers, R. J.; Smith, L. M. *J. Am. Chem. Soc.* **2000**, *122*, 1205−1209.
(27) Yu, W. H.; Kang, E. T.; Neoh, K. G.; Zhu, S. *J. Phys. Chem. B* **2003**, *107*, 10198−10205.
(28) Yu, W. H.; Kang, E. T.; Neoh, K. G. *Ind. Eng. Chem. Res.* **2004**, *43*, 5194−5202.
(29) Liu, Y.-J.; Navasero, N. M.; Yu, H.-Z. *Langmuir* **2004**, *20*, 4039−4050.
(30) Jin, H.; Kinser, R.; Bertin, P. A.; Kramer, D. E.; Libera, J. A.; Hersam, M. C.; Nguyen, S. T.; Bedzyk, M. J. *Langmuir* **2004**, *20*, 6252−6258.
(31) Gu, J.; Yam, C. M.; Li, S.; Cai, C. *J. Am. Chem. Soc.* **2004**, *126*, 8098−8099.
(32) Wei, F.; Sun, B.; Guo, Y.; Zhao, X. S. *Biosens. Bioelectron.* **2003**, *18*, 1157−1163.
(33) Cattaruzza, F.; Cricenti, A.; Flamini, A.; Girasole, M.; Longo, G.; Mezzi, A.; Prosperi, T. *J. Mater. Chem.* **2004**, *14*, 1461−1468.
(34) Sieval, A. B.; Linke, R.; Heij, G.; Meijer, G.; Zuilhof, H.; Sudhölter, E. J. R. *Langmuir* **2001**, *17*, 7554−7559.
(35) Lin, Z.; Strother, T.; Cai, W.; Cao, X.; Smith, L. M.; Hamers, R. J. *Langmuir* **2002**, *18*, 788−796.
(36) Lasseter, T. L.; Clare, B. H.; Abbott, N. L.; Hamers, R. J. *J. Am. Chem. Soc.* **2004**, *126*, 10220−10221.
(37) Hart, B. R.; Létant, S. E.; Kane, S. R.; Hadi, M. Z.; Shields, S. J.; Reynolds, J. G. *Chem. Commun*. **2003**, 322−323.
(38) Létant, S. E.; Hart, B. R.; Kane, S. R.; Hadi, M. Z.; Shields, S. J.; Reynolds, J. G. *Adv. Mater.* **2004**, *16*, 689−693.
(39) Böcking, T.; James, M.; Coster, H. G. L.; Chilcott, T. C.; Barrow, K. D. *Langmuir* **2004**, *20*, 9227−9235.
(40) Patole, S. N.; Pike, A. R.; Connolly, B. A.; Horrocks, B. R.; Houlton, A. *Langmuir* **2003**, *19*, 5457−5463.
(41) Errington, J.; Petkar, S. S.; Horrocks, B. R.; Houlton, A.; Lie, L. H.; Patole, S. N. *Angew. Chem., Int. Ed.* **2005**, *44*, 1254−1257.
(42) Pike, A. R.; Ryder, L. C.; Horrocks, B. R.; Clegg, W.; Connolly, B. A.; Houlton, A. *Chem. Eur. J.* **2005**, *11*, 344−353.
(43) Zhai, G.; Yu, W. H.; Kang, E. T.; Neoh, K. G.; Huang, C. C.; Liaw, D. J. *Ind. Eng. Chem. Res.* **2004**, *43*, 1673−1680.
(44) Coffinier, Y.; Olivier, C.; Perzyna, A.; Grandidier, B.; Wallart, X.; Durand, J.-O.; Melnyk, O.; Stiévenard, D. *Langmuir* **2005**, *21*, 1489−1496.
(45) Chidsey, C. E. D.; Bertozzi, C. R.; Putvinski, T. M.; Mujsce, A. M. *J. Am. Chem. Soc.* **1990**, *112*, 4301−4306.
(46) Chidsey, C. E. D. *Science* **1991**, *251*, 919−922.
(47) Hickman, J. J.; Ofer, D.; Zou, C.; Wrighton, M. S.; Laibinis, P. E.; Whitesides, G. M. *J. Am. Chem. Soc.* **1991**, *113*, 1128−1132.
(48) Rowe, G. K.; Creager, S. E. *J. Phys. Chem.* **1994**, *98*, 5500−5507.
(49) Weber, K.; Creager, S. E. *Anal. Chem.* **1994**, *66*, 3164−3172.
(50) Weber, K.; Hockett, L.; Creager, S. *J. Phys. Chem. B* **1997**, *101*, 8286−8291.
(51) Creager, S. E.; Wooster, T. T. *Anal. Chem.* **1998**, *70*, 4257−4263.
(52) Creager, S. E.; Rowe, G. K. *J. Electroanal. Chem.* **1997**, *420*, 291−299.
(53) Richardson, J. N.; Peck, S. R.; Curtin, L. S.; Tender, L. M.; Terrill, R. H.; Carter, M. T.; Murray, R. W.; Rowe, G. K.; Creager, S. E. *J. Phys. Chem*. **1995**, *99*, 766−772.
(54) Tender, L.; Carter, M. T.; Murray, R. W. *Anal. Chem.* **1994**, *66*, 3173−3181.
(55) Smalley, J. F.; Feldberg, S. W.; Chidsey, C. E. D.; Linford, M. R.; Newton, M. D.; Liu, Y.-P. *J. Phys. Chem.* **1995**, *99*, 13141−13149.
(56) Clegg, R. S.; Hutchinson, J. E. *J. Am. Chem. Soc.* **1999**, *121*, 5319−5327.
(57) Chambers, R. C.; Inman, C. E.; Hutchison, J. E. *Langmuir* **2005**, *21*, 4615−4621.
(58) Sek, S.; Misicka, A.; Bilewicz, R. *J. Phys. Chem. B* **2000**, *104*, 5399−5402.
(59) Bediako-Amoa, I.; Sutherland, T. C.; Li, C.-Z.; Silerova, R.; Kraatz, H.-B. *J. Phys. Chem. B* **2004**, *108*, 704−714.
(60) Orlowski, G. A.; Chowdhury, S.; Long, Y.-T.; Sutherland, T. C.; Kraatz, H.-B. *Chem. Commun.* **2005**, 1330−1332.
(61) Valincius, G.; Niaura, G.; Kazakeviciene, B.; Talaikyte, Z.; Kazemekaite, M.; Butkus, E.; Razumas, V. *Langmuir* **2004**, *20*, 6631−6638.
(62) Seo, K.; Cheol Jeon, I.; Yoo, D. J. *Langmuir* **2004**, *20*, 4147−4154.
(63) Yao, X.; Wang, J.; Zhou, F.; Wang, J.; Tao, N. *J. Phys. Chem. B* **2004**, *108*, 7206−7212.
(64) Liu, J.; Paddon-Row: M. N.; Gooding, J. J. *J. Phys. Chem. B* **2004**, *108*, 8460−8466.
(65) Smalley, J. F.; Sachs, S. B.; Chidsey, C. E. D.; Dudek, S. P.; Sikes, H. D.; Creager, S. E.; Yu, C. J.; Feldberg, S. W.; Newton, M. D. *J. Am. Chem. Soc.* **2004**, *126*, 14620−14630.
(66) Sikes, H. D.; Smalley, J. F.; Dudek, S. P.; Cook, A. R.; Newton, M. D.; Chidsey, C. E. D.; Feldberg, S. W. *Science* **2001**, *291*, 1519−1523.
(67) Sachs, S. B.; Dudek, S. P.; Hsung, R. P.; Sita, L. R.; Smalley, J. F.; Newton, M. D.; Feldberg, S. W.; Chidsey, C. E. D. *J. Am. Chem. Soc.* **1997**, *119*, 9, 10563−10564.
(68) Creager, S.; Yu, C. J.; Bamdad, C.; O'Connor, S.; MacLean, T.; Lam, E.; Chong, Y.; Olsen, G. T.; Luo, J.; Gozin, M.; Kayyem, J. F. *J. Am. Chem. Soc.* **1999**, *121*, 1059−1064.
(69) Brook, M. A. *Silicon in Organic, Organometallic, and Polymer Chemistry;* Wiley: New York, NY, 2000.
(70) Bateman, J. E.; Eagling, R. D.; Worrall, D. R.; Horrocks, B. R.; Houlton, A. *Angew. Chem., Int. Ed.* **1998**, *37*, 2683−2685.
(71) Kruse, P.; Johnson, E. R.; DiLabio, G. A.; Wolkow, R. A. *Nano Lett.* **2002**, *2*, 807−810.
(72) Dalchiele, E. A.; Aurora, A.; Bernardini, G.; Cattaruzza, F.; Flamini, A.; Pallavicini, P.; Zanoni, R.; Decker, F. *J. Electroanal. Chem*. **2005**, *579*, 133−142.
(73) Li, Q.; Mathur, G.; Gowda, S.; Surthi, S.; Zhao, Q.; Yu, L.; Lindsey, J. S.; Bocian, D. F.; Misra, V. *Adv. Mater.* **2004**, *16*, 133−137.
(74) Balakumar, A.; Lysenko, A. B.; Carcel, C.; Malinovskii, V. L.; Gryko, D. T.; Schweikart, K.-H.; Loewe, R. S.; Yasseri, A. A.; Liu, Z.; Bocian, D. F.; Lindsey, J. S. *J. Org. Chem.* **2004**, *69*, 1435−1443.
(75) Roth, K. M.; Yasseri, A. A.; Liu, Z.; Dabke, R. B.; Malinovskii, V.; Schweikart, K.-H.; Yu, L.; Tiznado, H.; Zaera, F.; Lindsey, J. S.; Kuhr, W. G.; Bocian, D. F. *J. Am. Chem. Soc.* **2003**, *125*, 505−517.
(76) Li, Q.; Mathur, G.; Homsi, M.; Surthi, S.; Misra, V.; Malinovskii, V.; Schweikart, K.-H.; Yu, L.; Lindsey, J. S.; Liu, Z.; Dabke, R. B.; Yasseri, A.; Bocian, D. F.; Kuhr, W. G. *Appl. Phys. Lett.* **2002**, *81*, 1494−1496.
(77) Higashi, G. S.; Chabal, Y. J.; Trucks, G. W.; Raghavachari, K. *Appl. Phys. Lett*. **1990**, 56, 656−658.
(78) Wade, C. P.; Chidsey, C. E. D. *Appl. Phys. Lett.*, **1997**, *71*, 1679−1681.
(79) Bäuerle, P.; Hiller, M.; Scheib, S.; Sokolowski, M.; Umbach, E. *Adv. Mater.* **1996**, *8*, 214−218.
(80) Linford, M. R.; Fenter, P.; Eisenberger, P. M.; Chidsey, C. E. D. *J. Am. Chem. Soc.* **1995**, *117*, 3145−3155.
(81) Sieval, A. B.; Vleeming, V.; Zuilhof, H.; Sudhölter, E. J. R. *Langmuir* **1999**, *15*, 8288−8291.
(82) Gassman, P. G.; Macomber, D. W.; Hershberger, J. W. *Organometallics* **1983**, *2*, 1470−1472.
(83) Woodbridge, C. M.; Pugmire, D. L.; Johnson, R. C.; Boag, N. M.; Langell, M. A. *J. Phys. Chem. B* **2000**, *104*, 3085−3093.
(84) Cicero, R. L.; Linford, M. R.; Chidsey, C. E. D. *Langmuir* **2000**, *16*, 5688−5695.
(85) Bard, A. J.; Faulkner, L. R. *Electrochemical Methods. Fundamentals and Applications;* Wiley: New York, NY, 1980; p. 522.
(86) Allongue, P.; Henry de Villeneuve, C.; Pinson, J. *Electrochim. Acta* **2000**, *45*, 3241−3248.
(87) Gonzalez, J.; Molina, A. *J. Electroanal. Chem.* **2003**, *557*, 157−165.
(88) Sze, S. M. *The Physics of Semiconductor Devices*, 2nd ed.; Wiley: New York, NY, 1981.
(89) Laser, D.; Bard, A. J. *J. Phys. Chem.* **1976**, *80*, 459−466.
(90) Cassie, A. B. D. *Discuss. Faraday Soc.* **1948**, *3*, 11−16.
(91) Sun, Q.-Y.; de Smet, L. C. P. M.; van Lagen, B.; Giesbers, M.; Thüne, P. C.; van Engelenburg, J.; de Wolf, F. A.; Zuilhof, H.; Sudhölter, E. J. R. *J. Am. Chem. Soc.* **2005**, *127*, 2514−2523.
(92) Laviron, E. *J. Electroanal. Chem*. **1979**, *101*, 19−28.
(93) (a) For v larger than ~50 V s^{-1}, we have noticed a deviation from linearity of the $E_p - \log v$ plots, which suggests that the data are not adequately fitted using the Laviron's formalism. The nonlinear dependence of peak potentials on $\log v$ is taken into account in the Marcus theory that incorporates potential-dependent α values.[46,93b] So, k_{app} can be extracted from working curves published by Murray and co-workers[93c] giving the dependence of E_p on $\log(v/k_{app})$ for various values of outer-sphere reorganization energies λ_{os} (eq 4)

$$\lambda_{os} = \frac{e^2 N}{8\pi\epsilon_0}\left[\frac{1}{a}\frac{1}{2d}\right] \times \left[\frac{1}{\epsilon_{op}}\frac{1}{\epsilon_s}\right] \quad (4)$$

where e is the electron charge, N Avogadro's number, ϵ_0 the permittivity of free space (8.8542×10^{-12} A s V^{-1} m^{-1}), a the molecular radius of the redox center, d the distance of the redox center from the electrode surface, ϵ_{op} and ϵ_s the optical and static dielectric constants of the medium around the redox center. For the ferrocene/ferrocenium system studied herein, λ_{os} is estimated at ~104 kJ mol^{-1}, i.e., 1.08 eV, with $a = 3.3$ Å,[45] $d = 26$ Å, ϵ_{op}=1.80, and ϵ_s=37.5 for CH_3CN[93d]. (b) Marcus, R. A. *J. Chem. Phys.* **1965**, *43*, 679−701. (c) Tender, L.; Carter, M. T.; Murray, R. W. *Anal. Chem.* **1994**, *66*, 3173−3181. (d) Gennett, T.; Milner, D. F.; Weaver, M. J. *J. Phys. Chem*. **1985**, *89*, 2787−2794.